Journal of Applied Sciences

ISSN 1812-5654

science alert

ANSInet
an open access publisher
http://ansinet.com

Journal of Applied Sciences 7 (23): 3687-3695, 2007
ISSN 1812-5654

Process Modelling of Ultrafiltration Units: An RSM Approach

[1]M.O. Daramola, [1]K.J. Keesman and [2]F. Spenkelink
[1]Systems and Control Group, Wageningen University, The Netherlands
[2]Norit Process Technology, Enschede, The Netherlands

Abstract: This study reports a study on the process modelling of ultrafiltration (UF) units with a focus on the development of backwashing models based on properly designed experiments under pilot scale conditions. For the modelling, series of experiments were designed using a star- 2^3 (fractional) factorial design methods and performed with the so-called SMART-XIGA pilot plant provided by Norit Membrane Technology, a key player in the membrane manufacturing. The influential factors on both the Hydraulic Backwash (HB) and Chemically Enhanced Backwash (CEB) are considered as variables in the resulting second-order regression models. The development and cross-validation of the models is solely based on the results obtained from the properly designed experiments. Explanation of the interactions among the considered factors was investigated via graphical and eigenvalue analysis using Response Surface Methodology (RSM) approach of empirical modelling. The results show that, a change in transmembrane pressure in HB is largely dependent on the backwash time and backwash frequency with backwash flux having no effect. Reversibility of the fouled layer in CEB is greatly dependent on the coagulant concentration dosing and the filtration flux and not so much on the filtration time. Also, the cross-validation and the ANOVA analysis carried out show that the models are valid in the region of our nominal working points.

Key words: Ultrafiltration, response surface methodology, hydraulic backwashing, chemically enhanced backwashing, modelling

INTRODUCTION

Separation and purification processes using membrane technology are gaining popularity in many chemical and food processing as well as in wastewater treating industries. The technology offers several advantages over and above the traditional techniques, including low energy requirement and low temperature operation (Sulaiman *et al*., 2001). The membrane separation and filtration processes, comprises a continuum of processes designed to separate particles or solute of different sizes by utilization of membranes containing appropriately sized pores (Ohya, 1976). The processes are Microfiltration (MF), Ultrafiltration (UF), Nanofiltration (NF) and Reverse Osmosis (RO) in order of decreasing pore size. A membrane has the ability to transport one component more readily than the other because of differences in physical and/or chemical properties between the membrane and the solute. Transport through the membrane occurs as a result of a driving force (pressure) and the permeation rate (flux), which is proportional to the force.

Meanwhile, this study focuses on UF and its applications in the treatment of water for irrigation purposes using dead-end mode because of its relative low energy consumption compared to the cross-flow mode (Kennedy *et al*., 1998; Katsikaris *et al*., 2005). UF has a pore size of about 0.01-0.1 μm and thus prevents particles, colloids, microorganisms and dissolved solids that are larger in dimension than the pores in the membrane surface from passing.

Ultrafiltration processes have been widely applied to a variety of fields. More specifically, in the area of industrial wastewater treatment, UF has been applied to tannery wastewaters in order to recycle trivalent chromium (Fabiani *et al*., 1996; Shaalan *et al*., 2001) or to remove colour from tannery wastewaters (Alves and De Pinho, 2000) in textile industry as a pre-treatment step prior to NF or RO for recycling and reuse of textile wastewaters (Marcucci *et al*., 2001) in olive-mill waster waters in combination with centrifugation for the reduction of organic polluting compounds (Turano *et al*., 2002) and even in the artificial kidney mechanisms (Serra *et al*., 1998). Therefore, the great extent of the UF in industrial operations generates the need of a useful tool for determination of membrane performance and indeed the minimization of the operating costs.

Membrane fouling and scaling, a major problem in membrane technology-based processes, affects the performance of the process and eventually damage the

Corresponding Author: Michael Daramola, Systems and Control Group, Wageningen University, The Netherlands

membranes. This hampers the economic viability for the development and spreading of the process (Reith and Birkenhead, 1998; Alonso *et al*., 2001). In clarification/filtration operations, deposits from fouling create an additional resistance to mass transfer (Serra *et al*., 1998). Fouling decrease would increase permeate flux and so proportionally reduce plant size and/or operating costs. However, fouling decrease depends on the method of removal such as backwashing, backflushing and so on. Therefore, there is a need to better understand UF process in term of the fouling mechanism and backwash effectiveness as it is presented in this paper. Accurate backwash modelling and optimization is very paramount to achieving greater backwash effectiveness. Thus reducing fouling.

Backwashing can either be Hydraulic Backwashing (HB) or Chemically Enhanced Backwashing (CEB) (Cheryan, 1998). During backwash, permeate flows back through the membrane, lifts off the cake and flushes it out of the module in dead-end mode. Each operating cycle is thus made up of a filtration phase followed by a backwash phase that allows the membrane to recover its initial properties. Meanwhile, this method of reversing the membrane properties (hydraulic backwash) does not lead to 100% recovery due to availability of some particles embedded within the membrane pores and fibres. To remove this, another form of backwash called Chemically Enhanced Backwash (CEB) is needed. Therefore, the effectiveness of cleaning procedures (HB and CEB) plays an important role in the performance of membranes (Heijman *et al*., 2007). However, these procedures require a break in the production process, use of chemicals and consumption of part of the permeate produced, thus reducing the productivity of the process and increasing the total operating costs with additional chemical costs, energy costs and waste water disposal costs.

Therefore to maximize productivity and minimize operating costs in UF, it is necessary to optimize the backwash process. However, optimizing this process depends on availability of accurate models that will adequately explain the inter-relationships/interactions among the influencing factors. However, some models have been developed for membrane filtration explaining the mechanisms of fouling especially ultrafiltration (Jaffin *et al*., 1997; Gaurdix *et al*., 2004; Heijman *et al*., 2007). Even Roling (2005) came up with a model which tries to measure the efficiency of CEB considering coagulant concentration dosing, filtration flux and the filtration time in a chemically enhance backwash. Meanwhile, the model is very cumbersome and will require a lot of time for model update as this is necessary since water quality changes periodically.

Nevertheless, studies by Kennedy *et al*. (1998), Kennedy (2006) and Roling (2005) resulted into identifying coagulant concentration dosing, CEB frequency, filtration time, filtration flux, soak time and backwash flux as factors influencing both hydraulic backwashing and chemically enhanced backwashing. Using physical modeling approach, a good starting point in studying the dynamic and thus optimizing a UF, to formulate an accurate backwash model has a disadvantage of many unknowns which invariably make such models complex. Consequently, the objective of this paper is to provide a methodology to find appropriate backwash models for further insight and optimization of the process. The methodology described in this paper employed empirical modeling approach (Box and Draper, 1987) which makes use of the experimental data with the accommodation of process data in the model if available and the need be.

EXPERIMENTAL DESIGN

This study employed (fractional) factorial designs for the experiments. These designs were adopted because of their relative goodness, as explained by Box and Hunter (Box and Hunter, 1961). A two-level factorial design was used for HB while this was extended to a star two-level fractional factorial design for (CEB). The use of the more advanced design for CEB was to reduce the number of experimental runs while still keeping a good coverage of the region around the nominal settings.

MATERIALS AND METHODS

The experiments were performed using SMART-XIGA pilot plant provided by Norit Membrane Technology, Enscede, The Netherlands (Fig. 1 for the process flow diagram of the plant and Fig. 4 for the photograph of the experimental set-up) containing an 8-inch polyether sulfone (PES) UF membrane module. The PES is a capillary hollow fibre type with an effective length of 25 cm and membrane area 0.0754 m^2 with a total of 120 fibres. The membrane, which is capable of inside-out filtration, was operated in dead-end mode. Chemicals used for CEB were NaOH solution of pH = 12.3 and HCl of pH = 2.3. The coagulant was an acidified solution of $FeCl_3$ prepared from a concentrated solution of $FeCl_3$ containing 14 wt% of Fe^{3+}. The coagulation pump (WATSON MARLOW 323) was calibrated experimentally to accommodate the desired flow for the in-line coagulation according to the experimental design for the CEB.

For hydraulic backwash, nine experimental runs were performed and the change in TMP (ΔTMP) in bar was estimated from:

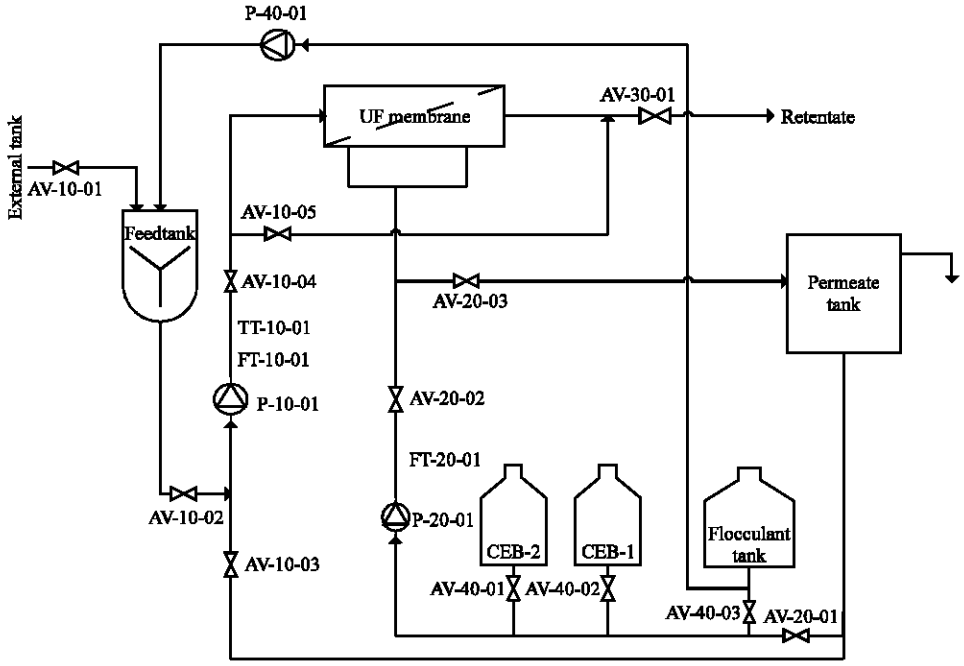

Fig. 1: The process flow diagram of the smart XIGA UF pilot plant. AV = Automatic valve, FT = Flow transmitter, TT = Temperature transmitter, P-10-01 = Feed pump, P-20-01 = Backwash pump, P-40-01 = Coagulation pump, CEB-1 = Tank containing diluted hydrochloric acid and CEB-2 = Tank containing NaOH solution

$$\Delta TMP = TMP_f - TMP_o \quad (1)$$

Where:

TMP_f = Final transmembrane pressure at the end of filtration, i.e., at $T_f = 20$ min,

TMP_0 = Transmembrane pressure of the membrane at the commencement of the filtration.

Furthermore, the following holds:

$$t_f = \frac{T_f}{B_f} - t_b \quad (2)$$

Where:

t_f = Filtration cycle time (min),

T_f = Total time for the filtration with time for hydraulic backwash inclusive,

B_f = Backwash frequency,

t_b = Backwash time (min).

The experimental range and coded factors used in the experimentation is presented in Table 1.

Reversibility of the fouling layer during CEB was estimated according to Roorda (2004) using:

Table 1: Experimental range and coded levels of the three independent variables for HB

Variables	Actual	Coded	Actual	Coded	Actual	Coded
Backwash frequency	2.0	-1	3	0	4.0	+1
Backwash time (min)	0.5	-1	1	0	1.5	+1
Backwash flux (l m^{-2} h^{-1})	150.0	-1	200	0	250.0	+1

$$R_x = \frac{(R_{h,n} - R_o) - (R_{CEB} - R_o)}{(R_{h,n} - R_o)} \times 100\% \quad (3)$$

However, $R_{h,n}$ was not easily determined from the experiments because the CEB rapidly starts immediately after the completion of the specified nth filtration. Therefore, based on the area observed, 100% effectiveness of the hydraulic backwash was assumed. The gradient of each filtration cycle (β_n) was calculated and averaged. The average value was used in the prediction of $R_{h,n}$ using the following relationship:

$$R_{h,n} = \beta_{av} * t_f + R_{h,n-1} \quad (4)$$

Where:

β_{av} = Average gradient (bar min^{-1}) over n-1 cycles.

The raw water used in the experimentation was the same as in the full-scale plant. Under the given

experimental conditions the resistance measured was very small to the extent that it was difficult to use the values in the model formulation. However, according to Cheryan (1998), resistance at a constant flux and viscosity can be expressed as:

$$R = \frac{TMP}{\mu * J} \quad (5)$$

Where:
R = Resistance during filtration (m^{-1}),
J = Filtration flux ($l\ m^{2}\ h^{-1}$),
μ = Viscosity ($Ns\ m^{-2}$).

If μ and J are constant and setting $TMP_{hCEB} = TMP_{h,n}$ for n = 10, substitution of Eq. 5 in 3 gives:

$$R_x = \frac{(TMP_{hCEB} - TMP_{CEB})}{(TMP_{hCEB} - TMP_o)} \times 100\% \quad (6)$$

Where:
TMP_{hCEB} = Transmembrane pressure after the hydraulic backwash before CEB commences (bar),
TMP_{CEB} = Transmembrane pressure after the CEB and TMP_{CEB} the transmembrane pressure before the start of filtration (bar). Hence from (6) and given the TMP profile, R_x can be calculated. Table 2 gives the experimental range and coded factors used in CEB experimentation.

Statistical analysis and modelling: For HB the proposed mathematical relationship between the independent variables and the response is given by:

$$\Delta TMP = \Delta TMP_o + \alpha_1 t_b + \alpha_2 B_f + \alpha_3 J_b + \alpha_4 t_b^{\,2} + \alpha_5 B_f^{\,2} + \alpha_6 J_b^{\,2} + \alpha_7 t_b J_b + \alpha_8 t_b B_f + \alpha_9 J_b B_f \quad (7)$$

Where:
ΔTMP = Predicted response,
ΔTMP_o = Intercept.

Furthermore, α_1,... α_9 denote the regression coefficients related to linear, quadratic and interaction terms.

For the CEB modelling, we propose the following second-order polynomial equation:

$$R_x = R_{xo} + \alpha_1 J_f + \alpha_2 t_f + \alpha_3 C_c + \alpha_4 J_f^{\,2} + \alpha_5 t_f^{\,2} + \alpha_6 C_c^{\,2} + \alpha_7 J_f t_f + \alpha_8 t_f C_c + \alpha_9 J_f C_c + \alpha_{10} J_f t_f C_c \quad (8)$$

Table 2: Experimental range and coded levels of the three independent variables for CEB

Variables	Actual	Coded	Actual	Coded	Actual	Coded
Filtration flux ($l\ m^{-2}\ h^{-1}$)	20	$-\sqrt{3}$	70	0	120	$+\sqrt{3}$
Filtration time (min)	20	$-\sqrt{3}$	62.5	0	120	$+\sqrt{3}$
Coagulant concentration dosing (ppm)	0	$-\sqrt{3}$	2.5	0	5	$+\sqrt{3}$

Where:
R_x = Predicted response,
R_{xo} = Intercept,
$\alpha 1$, ..., α_{10} = Regression coefficients.

Validation of the models: In order to determine the accuracy of the models, additional experimental runs were designed and performed at constant operating conditions. Cross-validation and ANOVA analysis (Daniel, 1977) were then carried out to further establish the validity of the models.

RESULTS

Modelling: The results obtained from the experiments were analysed and the regression coefficients calculated using ordinary least-squares estimation. As a result of this the following regression equations (with standard deviations of the estimated coefficients) are obtained

HB:

$$\Delta TMP = -0.020 - 0.512 t_b + 0.074 B_f - 0.015 B_f^{\,2} - 0.104 B_f t_b \quad (9)$$
$$(\pm 0.032)\ (\pm 0.472)\ (\pm 0.023)\ (\pm 0.004)\ (\pm 0.149)$$

CEB:

$$R_x = 102.2 + 0.562 J_f - 0.020 t_f - 31.75 C_c - 0.009 J_f^{\,2} - 1.127 C_c^{\,2} + 0.491 J_f C_c - 0.002 t_f C_c \quad (10)$$
$$(\pm 10.60)\ (\pm 0.150)\ (\pm 0.086)\ (\pm 4.815)$$
$$(\pm 0.009)\ (\pm 0.360)\ (\pm 0.042)\ (\pm 0.046)$$

Equation 9 reveals that backwash flux (J_b) has no effect at all on ΔTMP and thus allowing a significant model reduction when compared with Eq. 7. Furthermore, taking into account the standard deviation of the estimation errors, only B_f has a pronounced effect on ΔTMP. However, this may be different when the same experimental design is performed under different process conditions. Also, Eq. 10 excludes some terms, in particular the term with the squared filtration time and the interaction of the three influencing factors considered as

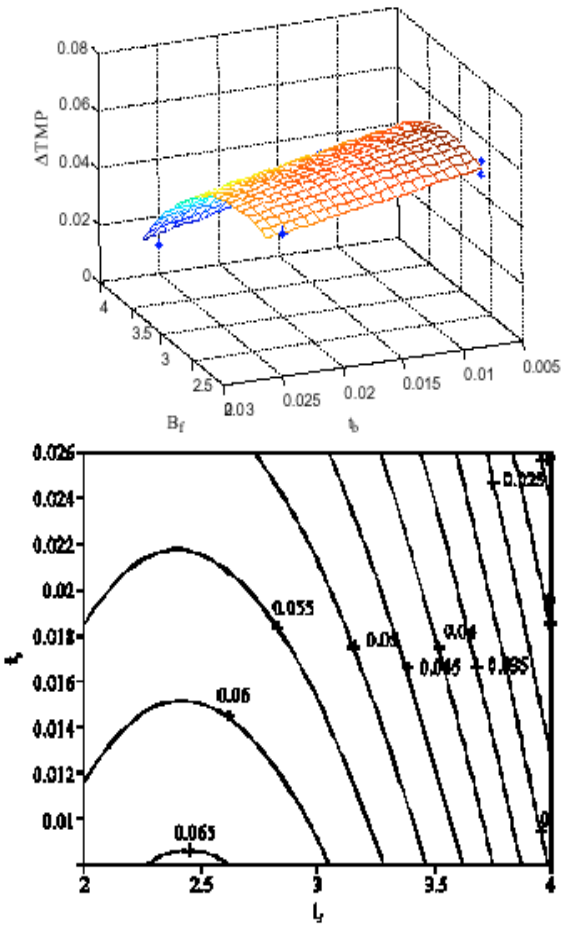

Fig. 2: Response surface (plus data points) and contour plot for HB

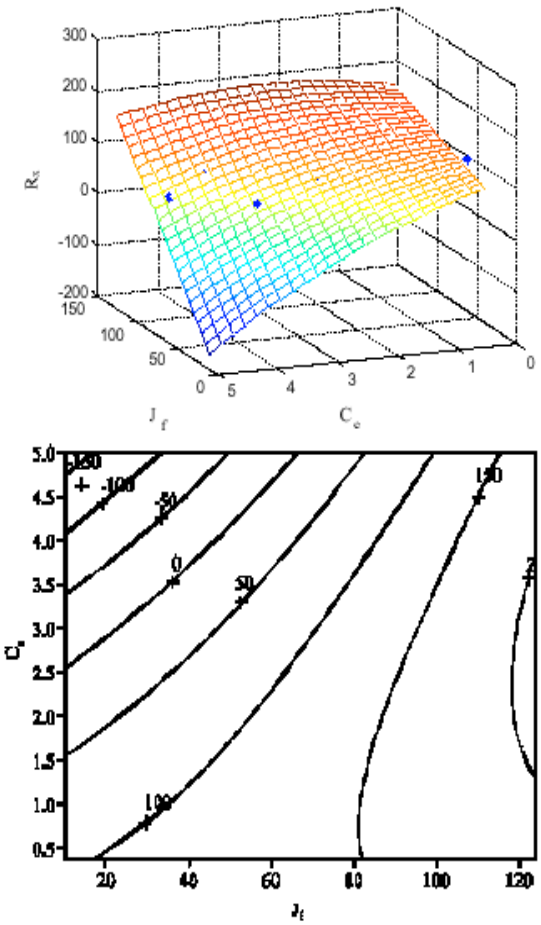

Fig. 3: Response surface (plus data points) and contour plot for CEB at $t_f = 62.5$ min

Table 3: Measured and predicted ΔTMP from the HB experiments using a 2^3 factorial design

S. No.	J_f(l m^{-2} h^{-1})	t_b(min)	B_f	ΔTMP (bar)	ΔTMP_n (bar)
1	0	0	0	0.054	0.054
2	-1	-1	-1	0.060	0.063
3	-1	-1	+1	0.028	0.030
4	-1	+1	-1	0.050	0.051
5	-1	+1	+1	0.010	0.014
6	+1	-1	-1	0.065	0.063
7	+1	-1	+1	0.031	0.031
8	+1	+1	-1	0.051	0.051
9	+1	+1	+1	0.018	0.014

*: see Table 1 for coded levels

Table 4: Measured and predicted R_e from the *CEB* experiments using a fractional factorial 2^3 + star design

S. No.	J_f (l m^{-2} h^{-1})	t_f (min)	C_e (ppm)	R_{es} (%)	R_{en} (%)
1	70.0	62.5	0.00	94.38	95.27
2	98.9	29.3	1.44	90.53	89.10
3	20.0	62.5	2.50	45.88	46.36
4	120.0	62.5	2.50	96.12	96.64
5	70.0	120.0	2.50	93.05	93.05
6	98.9	95.7	1.06	82.31	82.34
7	41.1	95.7	1.44	90.09	88.63
8	70.0	62.5	2.50	93.08	94.50
9	70.0	62.5	5.00	80.00	79.64

suggested in Eq. 8. Notice furthermore from Eq. 10 that the effect of t_f is questionable anyway. The HB regression model has a Mean Square Error (MSE) of 2.475×10^{-3}, while for the CEB regression model this was estimated to be 3.812. These values are the lowest among a large set of possible model candidates, which are obtained by setting one or more α's in Eq. 8 to zero. The measured responses and the model output responses obtained for HB and CEB are presented in Table 3 and 4, respectively.

Graphical interpretation: Figure 2 show the response surface and contour plot for the HB model Eq. 9 and Fig. 3 shows it for the CEB model Eq. 10. However, to understand the relationship among the influencing factors in CEB and given that t_f has very little effect, the model was evaluated at a fixed value of t_f. To allow a response surface analysis of the full model with three factors, which cannot be done graphically, Eq. 10 is written in vector-matrix notation,

$$R_x = R_{x0} + L^T \begin{bmatrix} J_f \\ t_f \\ C_c \end{bmatrix} + \begin{bmatrix} J_f & t_f & C_c \end{bmatrix} H \begin{bmatrix} J_f \\ t_f \\ C_c \end{bmatrix} \quad (11)$$

Where:

$$L = \begin{bmatrix} \alpha_1 \\ \alpha_2 \\ \alpha_3 \end{bmatrix} \text{ and } H = \begin{bmatrix} \alpha_4 & 0 & \frac{\alpha_5}{2} \\ 0 & 0 & \frac{\alpha_8}{2} \\ \frac{\alpha_5}{2} & \frac{\alpha_8}{2} & \alpha_6 \end{bmatrix}$$

Substituting the estimated coefficients of Eq. 10 and performing eigenvalue decomposition, i.e., $h = VDV^T$ with $V^TV = VV^T = I$ (identity matrix) and D a diagonal matrix gives:

$$V = \begin{bmatrix} -0.203 & 0.004 & -0.979 \\ 0.001 & 1 & 0.004 \\ 0.979 & 0 & -0.203 \end{bmatrix} \text{ and}$$

$$D = \begin{bmatrix} -1.178 & 0 & 0 \\ 0 & 0 & 0 \\ 0 & 0 & 0.060 \end{bmatrix}$$

These matrices indicate the shape and orientation of ellipsoidal contours (Abusam *et al*., 2001) for further explanation of ellipsoidal analysis). As a result of this, dominant directions on the response surface can be found. For instance, the first eigenvector (first column of V) with large corresponding eigenvalue D_{11} indicate a clear valley, more or less aligned with the axis of J_f. This is also confirmed by considering the third eigenvector and eigenvalue. Notice that, after equal scaling of the axis, this valley is also clearly visible in Fig. 3. The second eigenvector and eigenvalue indicate that t_f does not induce a curvature in the response surface.

In addition to this response surface analysis in higher dimensions, it is also possible to estimate extrema of the response surface, indicating optimal process conditions. For the CEB the optimum is given by:

$$-H^{-1} * \frac{L^T}{2} = 10^4 [0.0196 \quad 3.6354 \quad -0.0008] \quad (12)$$

Clearly, these steady state values are unrealistic and out of the applicability region. However, from Fig. 3 one can readily observe that approximately all linear combinations of J_f and C_c on the 100%-contour give an appropriate result in terms of R_x.

Fig. 4: Picture of the SMART-XIGA pilot plant used for experimentation

Table 5: Results of model validation for *HB* using again the 2^3 factorial design

S. No.	J_0(l m^{-2} h^{-1})	t_b (min)	B_f	ΔTMP (bar)	ΔTMP_p (bar)
1	0	0	0	0.036	0.054
2	+1	+1	+1	0.022	0.014
3	+1	+1	-1	0.044	0.051
4	+1	-1	+1	0.050	0.030
5	-1	+1	+1	0.013	0.014
6	-1	+1	-1	0.015	0.051
7	-1	-1	+1	0.032	0.030
8	+1	-1	-1	0.074	0.063
9	-1	-1	-1	0.080	0.063

*: see Table 1 for coded levels

Table 6: Result of model validation for CEB using the complementary fractional factorial 2^3 design

S. No.	J_f(l m^{-2} h^{-1})	t_f	C_c	R_x(%)	R_{xp}(%)
1	41.1	95.7	1.06	92.50	94.17
2	98.9	29.3	1.06	84.87	83.79
3	41.1	29.3	1.44	90.58	90.14
4	70.0	62.5	2.50	93.92	94.50

Validation of models: Table 5 and 6 present the results of cross-validation of the models. Table 5 shows that the predicted ΔTMP_p agrees fairly with the estimated R_x from the experimental data (MSE 0.18) and thus confirming the validity of the model. Also, Table 6 shows that the predicted reversibility R_{xp} and the estimated R_x are in fair agreement, with MSE 5.802.

In addition the ANOVA analysis of the two models presented in Table 7 and 8 shows $F_{0.995} = 18.63$ for HB model and $F_{0.995} = 16.24$ for CEB while their variance ratios (VR) are 0.001856 and 0.003278, respectively. According to Daniel (1977), since the VR values for both models are much more less that their respective F values, then this indicates that the models are reliable to explain the relationships investigated with the properly designed

Table 7: ANOVA analysis for HB model

Source of variation	SS	df (d_f)	MS	$F_{0.995}$	VR
Observation	8.89E-07	1	8.89E-07	18.63	3.278E-03
Error	0.99	0.94	4.789E-04		

Table 8: ANOVA analysis for CEB model

Source of variation	SS	df (d_f)	MS	$F_{0.995}$	VR
Observation	0.067	1	0.067	16.24	3.278E-03
Error	0.99	0.857	20.32		

experiments. Hence, there is a clear indication that the models are valid in the region of our nominal working points.

DISCUSSION

Small data sets: Depending on the process conditions, an individual experimental run can take several hours to more than one day. Hence, effective experimental designs must be chosen and thus usually small data sets are obtained. In our application on the influencing factors related to HB, 9 experimental runs (Table 1) were performed, while the number of regression coefficients is 5 (Eq. 9). Consequently, the error characteristics and especially the auto-correlation of the residuals, are difficult to evaluate and thus the standard deviations presented in Eq. 9 are only rough indications. As an alternative to the stochastic approach and most appropriate to small data sets, in the past a so-called set-membership or bounded-error approach has been proposed. In this approach it is assumed that the measurement error is bounded, so that effectively at each sample instant only intervals are considered instead of single points. For a full treatment of this approach we refer to e.g., (Walter, 2002; Norton, 2002; Keesman, 2002). In particular, for the linear estimation case exact solutions can be found. These exact solutions can be tightly bounded by boxes, which can be found by solving a couple of LP problems. Assuming an error bound on ΔTMP of 0.005; the following bounded (interval) estimates of the coefficients in Eq. 9 are found and presented in the second row of Table 9.

If the error bound is chosen too small no feasible solution will be found. Hence, there exists a minimum error bound for which the interval estimates reduce to a single point. This point estimate is called the min-max estimate. For our application, the min-max estimate of the coefficients is presented in the third row of Table 9. Notice that these min-max estimates are not too far from the least-squares estimates. The essence of this bounded-error approach is that now reliable uncertainty regions around the estimates are found.

Similar results have been found for the CEB case, but not presented here. Just notice that for the CEB model

Table 9: Bounded-error estimation results for HB

ΔTMP_0	α_1	α_2	α_3	α_4
[-0.081 0.042]	[-1.62 0.60]	[0.028 0.119]	[-0.023 -0.007]	[-0.45 0.24]
-0.022	-0.518	0.076	-0.015	-0.114

only 11 experimental runs, using a fractional factorial + star design, were performed while potentially for the second-order regression model Eq. 8, 10 coefficients were estimated. Consequently, 11 experimental runs are about the minimum, resulting in relatively high estimation errors. Nevertheless, the four cross-validation experiments (Table 6) indicate that the resulting CEB model (10) is reliable.

Prior physical knowledge: Notice from the contour plot of Fig. 2 that the model predicts a small decrease of ΔTMP when B_f is smaller than 2.5. This is a rather unlikely phenomenon. If there is sufficient evidence that the maximum should be at $B_f = 2$, then this information can be easily incorporate into the empirical modelling approach.

$$\text{Setting } \left.\frac{\partial \Delta TMP}{\partial B_f}\right|_{B_f=2} = 0$$

where the derivative can be easily found from Eq. 9, leads to the following constraint between α_2 and α_3: $\alpha_2 + 2\alpha_3 B_f = 0$, so that $\alpha_2 = -4\alpha_3$. Hence, after substitution of this relationship, the model structure of Eq. 9 becomes:

$$\Delta TMP = \Delta TMP_O + \alpha_1 t_b + \alpha_3(-4B_f + B_f^2) + \alpha_4 t_b B_f \quad (13)$$

in which the coefficients have to be re-estimated.

Hydraulic backwashing modelling: In Fig. 2 as the t_b increases, the ΔTMP linearly decreases. It can be explained that the longer the time for backwashing, the lower the change in the TMP. This shows a good removal of the fouled layer. Meanwhile, it is expected that for $t_b \rightarrow 0$, ΔTMP will become very high, indicating a hyperbolic relationship. Notice, however, that the experimental data (Table 3, 5) only support a linear relationship. Therefore, most likely the relationship between ΔTMP and t_b is inverse proportionality. However, this can only be verified through additional experimental runs to get more data points beyond the region considered in this study. Nevertheless, this is in agreement with the findings of earlier research (Roling, 2005; Kennedy *et al*., 1998; Kennedy, 2006; Delgado *et al*., 2004).

Figure 2 also shows that as the backwash frequency B_f increases from 2 to 4, ΔTMP decreases quadratically with increase of B_f. It can be explained that at low frequencies, there is more formation of cake layer than can

be removed with backwash. But as the frequency increases, the cake layer is washed off the membrane. Thus restoring the original property of the membrane. Therefore, the model shows that the higher the number of frequency of hydraulic backwash, the lower the ΔTMP. Thus the higher the rate of recovery of the flux.

Chemical enhanced backwashing modelling: First of all, it is good to notice that $0 \geq R_x \geq 100$. Figure 3 describes that the reversibility decreases non-linearly with an increase in the coagulant concentration dosing but increases non-linearly (almost linear) with an increase in the filtration flux. The decrease with respect to increased coagulant concentration dosing can be attributed to the more deposited particles as a result of coagulation action on the membrane. Thus providing more particles for possible blockage of the pores which is in tune with explanation of fouling mechanism in the studies of previous researchers Jaffin *et al.* (1997) and Gaurdix *et al.* (2004). In addition to this, the increase of R_x as a result of an increase in the filtration flux can be attributed to the fewer blockages of the membrane pores by the cake/coagulated particles as a result of high filtration flux. Thus making CEB more effective.

CONCLUSIONS

In this study, models for hydraulic backwashing and chemically enhanced backwashing have been developed and cross validated using an empirical modelling approach, in particular the Response Surface Methodology (RSM) (Box and Draper, 1987). The modelling was based on experimental data from the SMART-XIGA pilot plant, using modified factorial designs to limit the number of experimental runs, with the aim to study the full behaviour and the possibilities for optimization of UF plants. Cross-validation and ANOVA analysis led to the conclusion that the models are reliable under the given experimental conditions. The models showed that HB is largely influenced by backwash time and backwash frequency with backwash flux having no effect. The CEB depends largely on the coagulant concentration dosing and the filtration flux and not so much on the filtration time. For further implementation in practice, due to changes in e.g., the feed water quality, a regular update of the models is necessary and can be easily obtained using the methodology presented in this study.

ACKNOWLEDGMENTS

We want to acknowledge WMD/WLN and NORIT Membrane Technology situated in The Netherlands for the opportunity given and support in cash and kind in carrying out this study successfully.

NOMENCLATURE

B_f	=	Backwash frequency.
C_c	=	Coagulant concentration closing (ppm).
CEB	=	Chemically enhanced backwash.
HB	=	Hydraulic backwash.
J_b	=	Backward flux ($l\ m^{-2}\ h^{-1}$).
J_f	=	Filtration flux ($l\ m^{-2}\ h^{-1}$).
MSE	=	Mean square error.
n	=	No. of filtration cycle before CEB.
R_{CEB}	=	Resistance of the membrane after CEB (m^{-1}).
$R_{h,n}$	=	Resistance after hydraulic backwash at the end of n filtration cycle (m^{-1}).
R_o	=	Initial resistance of the membrane before filtration (m^{-1}).
ΔR_{fo}	=	Resistance of fouling layer after UF of feed water without cleaning (m^{-1}).
R_x	=	Reversibility of the fouling layer as a function of the cleaning procedure (%).
t_b	=	Backwash time (min).
t_f	=	Filtration time (min).
TMp_f	=	Transmembrane pressure at the end of the n filtration cycle (bar).
TMP_{hCEB}	=	Transmembrane pressure after the hydraulic backwash before CEB commences (bar).
TMP_o	=	Initial TMP before UF (bar).
ΔTMP	=	Change in transmembrane pressure (bar).
α_i	=	Coefficient in second-order regression model
β_{av}	=	Average gradient (bar min^{-1}).
μ	=	Dynamic viscosity (Nsm^{-2}).
SSTR	=	Treatment sum of squares.
VR	=	Variance ratio.
MSTR	=	Treatment mean squares.
SST	=	Total sum of squares.
SSE	=	Error sum of squares.
SS	=	Sum of squares.
MS	=	Mean squares.
d_f	=	Degree of freedom.

REFERENCES

Abusam, A., K.J. Keesman, G. Van Straten, H. Spanjers and K. Meinema, 2001. Sensitivity analysis in oxidation ditch modelling: The effect of variations in stoichiometric, kinetic and operating parameters on the performance indices. J. Chem. Technol. Biotechnol., 76: 430-438.

Alonso, E., A. Santos, G.J. Solis and P. Riesco, 2001. On the feasibility of urban wastewater tertiary treatment by membranes: A comparative assessment. Desalination, 141: 39.

Alves, A.M.B. and M.N. De Pinho, 2000. Ultrafiltration for colour removal of tannery dyeing wastewaters. Desalination, 130: 147-154.

Box, G.E.P. and J.S. Hunter, 1961a,b. The 2^{k-p} fractional factorial designs, I. Technometrics, 3: 311-351.

Box, G.E.P. and N.R. Draper, 1987. Empirical Model-Building and Response Surfaces. Wiley and Sons, USA., pp: 1-3.

Cheryan, M., 1998. Ultrafiltration and Microfiltration Handbook. Technomic Publishing Company, Lancaster, Pennsylvania.

Daniel, W.W., 1977. Introductory Statistics with Applications. Houghton Mifflin Company, USA.

Delgado, S., F. Diaz, L. Vera, R. Diaz and S. Elmaleh, 2004. Modelling hollow-fibre ultrafiltration of biologically treated wastewater with and without gas sparging. J. Membr. Sci., 228: 53-65.

Fabiani, C., F. Ruscio, M. Spadoni and M. Pizzichini, 1996. Chromium (III) salts recovery process from tannery wastewaters. Desalination, 108: 183-191.

Gaurdix, A., E. Sorensen, L.G. Papageorgiou and E.M. Guardix, 2004. Optimal design and operation of continuous ultrafiltration plants, J. Membr. Sci., 235: 131-138.

Heijman, S.G.J., M. Vantieghem, S. Raktoe, J.Q.J.C. Verberk and J.C. Van Dijk, 2007. Blocking of capillaries as fouling mechanism for dead-end ultrafiltration. J. Membr. Sci., 287: 119-125.

Jaffin, M.Y., L.H. Ding, Convreur, Ch. and P. Khari, 1997. Effect of ethanol on UF of Bovine Albumin solutions with organic membranes. J. Membr. Sci., 124: 233.

Katsikaris, K., C. Boukouvalas and K. Magoulas, 2005. Simulation of ultrafiltration process ad application to pilot tests. Desalination, 171: 1-11.

Keesman, K.J., 2002. Nonlinear-Model Case in Bound-Based Identification, in Control Systems, Robotics and Automation. In: Encyclopedia of Life Support Systems (EOLSS), Unbehauen, H. (Ed.). Developed under the auspices of the UNESCO, Eolss Publishers, Oxford, UK (http://www.eolss.net).

Kennedy, M., S.M. Kim, I. Mutenyo, L. Broens and J. Schippers, 1998. Intermittent cross flushing of hollow fibre UF systems. Desalination, 118: 175.

Kennedy, M., 2006. Fouling in MF and UF systems, in shortcourse on membrane technology in drinking and industrial water treatment. UNESCO-IHE, The Netherlands.

Marcucci, M., G. Nosenzo, G. Capannelli, I. Ciabatti, D. Corrieri and G. Ciardelli, 2001. Treatment and re-use of textile effluents based on new ultrafiltration and other membrane technologies. Desalination, 138: 75-82.

Norton, J.P., 2002. Linear-Model Case in Bound-based Identification, in Control Systems, Robotics and Automation. In: Encyclopedia of Life Support Systems (EOLSS), Unbehauen, H. (Ed.). Developed under the auspices of the UNESCO, Eolss Publishers, Oxford, UK (http://www.eolss.net).

Ohya, H., 1976. Reverse osmosis and ultrafiltration. Vol. I, Theory, Saiwai-Shobo.

Reith, C. and B. Birkenhead, 1998. Membranes enabling the affordable and cost effective reuse of wastewater as an alternative water source. Desalination, 177: 203

Roling, A.J., 2005. Flocculation and recovery: Optimalisatie van coagulantdosering. Thesis, report, Saxion Hopeschool, Enschede, The Netherlands.

Roorda, J.H., 2004. Filtration characteristics in dead-end ultrafiltration of WWTP-effluent. Ph.D Thesis, TUDelft, Netherlands.

Serra, C., M.J. Clifton, P. Moulin, J. Rouch and P. Aptel, 1998. Dead-end ultrafiltration in hollow fibre modules: Module design and process simulation. J. Membr. Sci., 145: 159-172.

Shaalan, H.F., M.H. Sorour and S.R. Tewfik, 2001. Simulation and optimization of a membrane system for chromium recovery from tanning wastes. Desalination, 141: 315-324.

Sulaiman, M.Z., N.M. Sulaiman and B. Abdellah, 2001. Prediction of dynamic permeate flux during cross-flow ultrafiltration of polyethylene glycol using concentration polarization-gel layer model. J. Membr. Sci., 189: 151-165.

Turano, E., S. Curcio, M.G. De Paola, V. Calabro and G. Iorio, 2002. An integrated centrifugation-ultrafiltration system in the treatment of olive mill wastewater. J. Membr. Sci., 209: 519-531.

Walter, E., 2002. Bound-Based Identification, in Control Systems. Robotics and Automation. In: Encyclopaedia of Life Support Systems (EOLSS), Unbehauen, H. (Ed.). Developed under the auspices of the UNESCO, Eolss Publishers, Oxford, UK. (http://www.eolss.net).